PHYSICAL REVIEW B VOLUME 33, NUMBER 3 1 FEBRUARY 1986

Surface ferromagnetism of Cr(001)

C. L. Fu and A. J. Freeman
Department of Physics and Astronomy, Northwestern University, Evanston, Illinois 60201

(Received 4 February 1985)

Results of self-consistent all-electron local- (spin-) density-functional studies of the electronic and magnetic properties of a seven-layer Cr(001) film are reported using our full-potential linearized augmented-plane-wave method. In agreement with earlier theoretical studies and recent photoemission experiments, a ferromagnetic Cr(001) surface is confirmed but with an associated surface magnetic moment of $2.49\mu_B$. The origin of the surface ferromagnetism is related to the sharp surface density-of-states peak near the Fermi level for the paramagnetic state. The calculated work function for the ferromagnetic state is found to be 4.05 eV—some 0.4 eV lower than that for the paramagnetic state; the difference indicates the importance of the magnetic order on this electrostatic quantity. In agreement with photoemission experiments, we find a prominent majority-spin surface state with a binding energy of 1 eV at the $\bar{\Gamma}$ point. Layer-by-layer contact hyperfine fields are evaluated: The core contributions are proportional to the magnetic moment of the corresponding atom, and the conduction-electron contribution shows a Friedel oscillation near the center layer. The contact hyperfine field for the surface atoms is also enhanced in magnitude, and a value of -73 kG is predicted.

I. INTRODUCTION

Surface magnetism of $3d$ transition metals has emerged as a field of increasing theoretical and experimental interest. Particular efforts include the effects on magnetism of reduced dimensionality and the possibility of ferromagnetic ordering on the surface of otherwise paramagnetic or antiferromagnetic bulk crystals. These questions have invoked considerable theoretical attempts to investigate and describe the electronic structure and the role played by surface states on these surface-related magnetic properties. One notable development for highly precise studies has been the all-electron full-potential linearized augmented-plane-wave (FLAPW) method[1] for solving the local- (spin-) density equations self-consistently for a single-slab geometry. In both[2] Ni(001) and[3] Fe(001), FLAPW calculations found no magnetically "dead" surface layers, in contrast to early experimental reports;[4] instead, an enhancement of the surface magnetic moment was predicted ($0.68\mu_B$ and $2.95\mu_B$, respectively). By contrast, the paramagnetic state of V(001) tends to be more stable[5] than the ferromagnetic state, and the occurrence of a reported[6] ferromagnetic phase transition is explained in terms of surface oxygen or impurity-induced surface reconstruction.[5]

Intense interest exists in the Cr(001) surface because of (1) the possibility of induced ferromagnetism in its surface layer while retaining antiferromagnetic behavior in the bulk;[7–15] and (2) the intriguing surface electronic structure of the (001) surface for the group-VIB transition, in general, and possible phenomena associated with the high density of states which arises from localized surface-state bands near the Fermi level, in particular. For[16] W(001) and Mo(001) the surface-state coupling plays a dominant role in the structural phase transition to the $c(2\times2)$ structure, whereas for Cr(001) the relatively narrow $3d$ surface-state band favors a large enhancement of the local-spin susceptibility. For these reasons, one might expect ferromagnetic ordering in the surface layer of Cr(001).

The existence of a ferromagnetic surface layer in antiferromagnetic chromium was first reported with the observation of surface magnetoplasma waves via an attenuated total reflection method[7] on polycrystalline chromium films. It has also been reported[8] that in small particles of chromium magnetic ordering persists well above the Néel temperature at 310 K. Recently, an electron-capture-spectroscopy study by Rau and Eichner[9] further confirmed the existence of ferromagnetic order below ~ 365 K, but with a $c(2\times2)$ reconstructed surface. Meier *et al.*[10] found no indication of ferromagnetism in spin-polarized photoemission studies from a chromium surface which, as they noted, included coverage of a nitrogen monolayer on top of the surface. It was later confirmed by low-energy electron diffraction (LEED) analyses[11] that the $c(2\times2)$-Cr(001) structure is related to surface impurities such as C, N, O, or S, and that a clean surface exhibits a $p(1\times1)$ LEED pattern at room temperature. Very recently, a surface magnetic phase transition was observed on Cr(001) using angle-resolved photoelectron spectroscopy (ARPES) by Klebanoff *et al.*:[12] From the temperature dependence of the splitting of the surface resonance state, the transition temperature was found to be 780 K; the exchange splitting interaction was estimated to be 0.8 eV at room temperature with an associated surface magnetic moment of $2.4\mu_B$. These findings are supported by the studies of Zajac *et al.*[17] on the epitaxy and electronic structure of Cr overlayers deposited on single-crystal Au(001).

Although the surface magnetism of Cr(001) seems well characterized, an *ab initio* theoretical study of the interplay between surface states and surface magnetism has not yet been undertaken. Earlier, a theoretical tight-binding-model study by Allan[13] predicted a ferromagnetic surface with a magnetic moment of $2.8\mu_B$ per surface atom. Using finite-temperature spin-fluctuation theory, Grempel[14] predicted the persistence of surface ferromagnetic order up to 900 K. Spin-polarized self-consistent electronic structure calculations on a five-layer $p(1\times1)$-Cr(001) slab by Hirashita *et al.*[15] using the linear combination of atomic orbitals—discrete variation (LCAO-DVM) method estimated the magnetic moment on the surface, second, and center layers to be $2.57\mu_B$, $-0.96\mu_B$, and $0.64\mu_B$, respectively.

In this paper we present results of a highly precise self-consistent, all-electron local-spin-density-functional study of a seven-layer Cr(001) slab by the FLAPW method. In Sec. II calculational models are briefly described. Results on the charge density, magnetic moment, and spin density including the hyperfine contact field are presented in Sec. III A. The one-particle energy spectra are discussed in Sec. III B with particular regard to the role played by the surface states in the surface ferromagnetic phase transition.

II. CALCULATIONAL MODEL

The Cr(001) surface is represented by a single slab consisting of seven atomic layers. No surface relaxation is considered in this study: Hence all nearest-neighbor distances are equal to $2R_{\mathrm{MT}}$ were $R_{\mathrm{MT}}=(\sqrt{3}/4)a$ is the radius of touching muffin-tin (MT) spheres, and a is the experimental bulk-lattice constant of 5.45 a.u. For the exchange-correlation potential we employ the explicit form of von Barth and Hedin[18] with the Hedin-Lundqvist[19] potential for the paramagnetic case.

The local-density equations are solved self-consistently by use of the FLAPW method[1] for a general potential, i.e., no shape approximations are made to the potential or charge density. All the matrix elements corresponding to this general potential are rigorously taken into account including, in particular, the nonspherical terms inside the MT spheres. All core electrons are treated fully relativistically, and the valence states (originating from the atomic $4s$ and $3d$ orbitals) are calculated semirelativistically.[20] These procedures allow an accurate description of the spin density at the nucleus (hyperfine contact field), which depends not only on the contribution from valence electrons but also on the dominant exchange polarization of the core electrons.[21]

Integrations over the first Brillouin zone (BZ) are based on a grid of 28 k points in the $\frac{1}{8}$ irreducible wedge of the two-dimensional BZ. A total number of 450 augmented plane waves are used as a variational basis set, split into two blocks (of about 225 basis functions each) using the mirror-plane reflection symmetry with respect to the center layer of the seven-layer slab (z reflection). With the MT sphere, the charge density and potential are expanded into lattice harmonics with an angular momentum component up to $l=8$. Self-consistency is assumed when the root-mean-square difference between the input and output charge densities and spin densities is less than 2×10^{-4} electrons/(a.u.)^3.

III. RESULTS AND DISCUSSION

A. Charge and spin densities

We start with the discussion of the charge density, since it is the central quantity in local-density-functional theory. The self-consistent valence charge density in the (110) plane of the upper half of a seven-layer Cr slab is shown in Fig. 1. Because of the short screening length induced by the metal-vacuum boundary, the charge density in the subsurface layer ($S-1$) exhibits the same contours as do those for the inner layers ($S-2$ and C). Further insight into the physical process of surface formation can be obtained from the total amount of valence charge within each MT sphere (cf. Table I): Notice the consistency of the charge within each MT sphere except for the surface atom—an amount of 0.3 electrons is transferred into the vacuum region. This charge spill-out, coming from the p-like electrons, serves to heal the surface discontinuity and determines the surface electrostatic dipole layer and thus the work function.

A spin-polarized FLAPW calculation of the Cr(001)

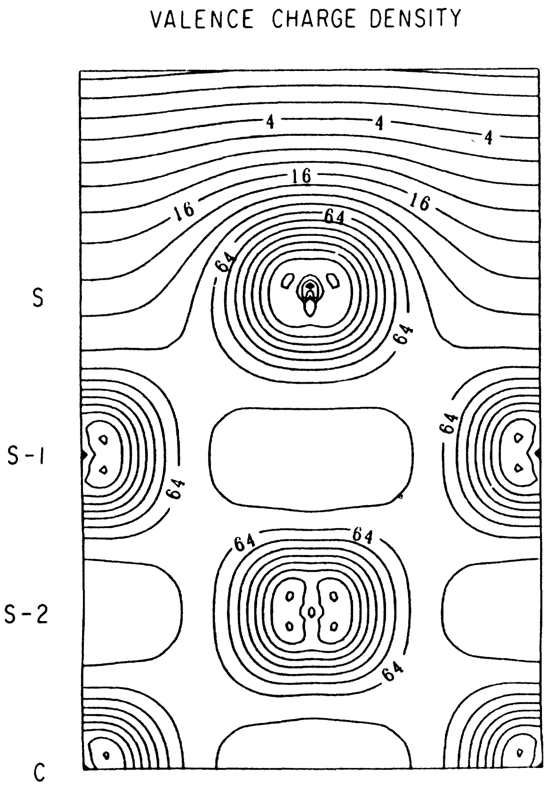

FIG. 1. Valence electronic charge density on the (110) plane for the seven-layer Cr(001) film in units of 1×10^{-3} electrons/(a.u.)^3. Subsequent contour lines differ by a factor of $\sqrt{2}$.

TABLE I. Theoretical work function and layer-by-layer MT valence electronic charge (in electrons) and magnetic moments (μ_B) for the seven-layer Cr(001) from the surface (S) to the center (C) layer of the film.

	S	$S-1$	$S-2$	C	Work function (eV)	
Paramagnetic					4.40	
Charge	4.66	4.93	4.94	4.95		
Ferromagnetic					4.05	
Charge	4.67	4.95	4.95	4.95		
Magnetic moment	2.49	−1.29	0.89	−0.89		
Experiment						
Magnetic moment	2.4[a]			0.59[b]		
Work function (eV)					4.10[c]	4.46[d]

[a] Reference 12.
[b] Reference 23.
[c] Reference 10.
[d] Reference 22.

surface gives a value of 4.05 eV for the work function. While this theoretical value is 0.4 eV lower than the experimental value obtained by Wilson and Mills[22] (4.46 eV), it is closer to the photoemission result by Meier *et al.*[10] (4.10±0.05 eV). Although both experiments claimed to stand for the work function of the clean Cr(001) surface, the agreement with the latter may be fortuitous, owing to the presence of one monolayer of nitrogen and zero spin polarization on their $p(1\times1)$ surface. On the other hand, it should be noted that the often-quoted experimental value (4.46 eV) of Ref. 22 refers to a surface contaminated by a submonolayer of impurities (O, S, and N) with a $c(2\times2)$ reconstructed structure. Thus, these experimental values cannot be regarded as the work function of a clean Cr(001) surface. Table I lists the work function and valence charge within each MT sphere for the ferromagnetic state as well as for the paramagnetic Cr(001) surface. The difference in work function (0.35 eV) between the paramagnetic and ferromagnetic states demonstrates the effect of magnetic order on a sensitive electrostatic quantity like work function; similar to the case of[3] Fe(001), the formation of magnetic order on the surface is accompanied by a decrease of the work function.

The spin density for the seven-layer Cr(001) film, shown in Fig. 2, exhibits antiferromagnetic coupling between adjacent layers in the [001] direction. The plot reveals highly anisotropic components of the spin density around the atomic sites with an essentially bulklike feature for the $S-2$ and C layers. The eruption of the spin density into the vacuum region is entirely positive and indicates a large enhancement of the magnetic moment at the surface. The induced ferromagnetic state has layer-projected magnetic moments within each MT sphere from the center to the surface layer given in Table I as $-0.89\mu_B$, $0.89\mu_B$, $-1.29\mu_B$, and $2.49\mu_B$. This surface-induced magnetic moment of $2.49\mu_B$ is comparable with earlier theoretical results obtained from the tight-binding method[14] ($2.8\mu_B$), and a DVM-LCAO calculation[15] ($2.56\mu_B$). In addition, our calculation shows that the spin polarization approaches its bulk value only two atomic layers beneath the surface. (For bulk Cr, the measured maximum magnetic moment at low temperature is $0.59\mu_B$).[23] The small increase of the calculated magnetic moment for center layer compared to its bulk value is apparently not due to a finite film size effect (cf. the constancy of the magnetic moment for the C and $S-2$ layers); instead it is due to the use of the experimental value of lattice constant in this calculation. It is now well recognized that LDF theory tends to give smaller equilibrium lattice constants (~3%) than experiment for $3d$

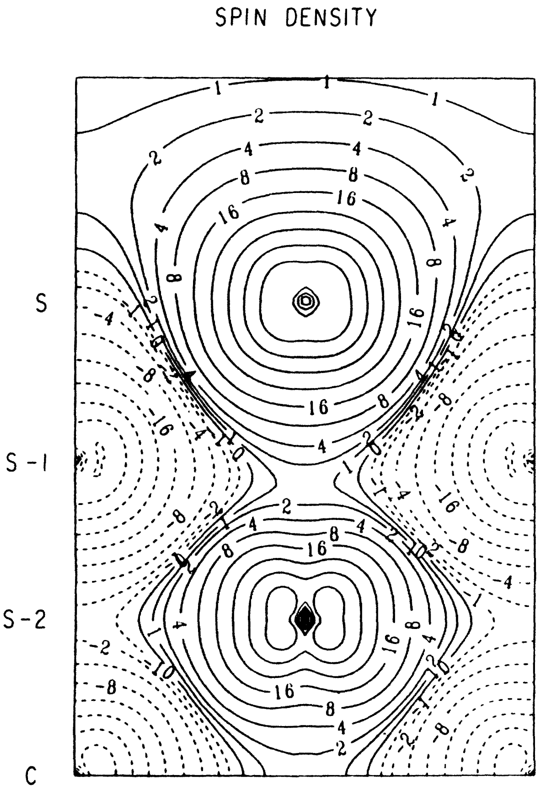

FIG. 2. Spin-density map on the (110) plane for the seven-layer Cr(001) film in units of 1×10^{-3} electrons/(a.u.)^3. Subsequent contour lines differ by a factor of 2.

TABLE II. Decomposition of the magnetic moment (in μ_B) by layer and l value in a seven-layer Cr(001) film.

	s	p	d	Total
C	-0.01	0	-0.89	-0.89
$S-2$	0.01	-0.01	0.90	0.89
$S-1$	-0.01	-0.01	-1.27	-1.29
S	0.03	0.02	2.44	2.49

transition metals; consequently, the calculated magnetic moment at the experimental lattice constant (which is dilated with respect to the value of LDF theory) tends to be larger. This lattice-constant-dependent behavior is even more sensitive for bulk Cr,[24,25] since Cr metal is close to the non-magnetic phase transition.

The decomposition of the magnetic moment inside the MT spheres by angular momentum and by layers is given in Table II. The increase of the magnetic moment in the surface region is mainly due to the imbalance of the majority- and minority-spin d-like electrons within each MT sphere; the contribution from delocalized s- and p-like electrons is only a few percent of the moment.

Consider now the spin densities at the nuclei for the seven-layer Cr(001) slab, which gives the contact polarization hyperfine field (H_{cf}). As shown in Table III, the total spin density at the nucleus is found to be of opposite sign to the corresponding magnetic moment for all layers. The total hyperfine field can be conveniently decomposed into two components for transition metals:[21] (1) a negative polarization of the core s electrons due to the d moment, and (2) the contribution from valence s-like electrons. The core part, as is now expected[21] even for metals, scales very precisely with the moment within each MT sphere (cf. last column in Table III). On the other hand, the valence contribution comes from the direct polarization of s-like electrons. Because of the cancellation effect between these two contributions, H_{cf} approaches zero for the center layer. On the other hand, an increase in magnitude of H_{cf} if found for the surface atom and is predominantly due to the large core contributions (from the magnetic moment enhancement) at the surface. Since the valence contribution to H_{cf} is not yet constant in the middle of the film, finite film size effects on H_{cf} cannot be completely excluded from our calculation. Despite this, a three-layer Cr(001) slab already yields an H_{cf} value for the surface atom (shown in the parentheses of Table III) which is identical to that of a seven-layer slab. The predicted value, -73 kG, for the surface atoms should be experimentally measurable.

TABLE III. Electronic spin densities at the nuclei in a seven-layer Cr(001) film in units of kG. The last column shows the ratio of the core spin density at the nucleus and the magnetic moment in the corresponding MT sphere (kG per unpaired spin). Numbers in parentheses are results for a three-layer Cr(001) film.

	Hyperfine field (kG)			
	Core	Valence	Total	$H_{cf}(\text{core})/M$
S	-328	256	-72	131
	(-352)	(279)	(-73)	
$S-1$	163	-140	23	126
$S-2$	-113	75	-38	127
C	113	-115	-2	127

B. One-particle energy spectra

The study of the density of states (DOS) decomposed into layers and l-like components gives insight into the mechanism of the surface-induced enhancement of the magnetism. In Fig. 3 we present the local DOS (LDOS) of the center [Fig. 3(a)] and surface layer [Fig. 3(b)] for a seven-layer paramagnetic Cr(001) film. The LDOS for the center layer is bulklike with the Fermi level (E_F) located in the valley separating the bonding and antibonding regions. This bulklike feature is persistent even for the $S-2$ layer—hence, an antiferromagnetic coupling between C and $S-2$ atoms with a magnetic moment close to its bulk value is obtained. A dramatic change of the surface LDOS from its bulk counterpart is seen in Fig. 3(b). Due to the reduced coordination number and the lower symmetry at the surface, there is an enchancement of the LDOS at E_F. This high DOS at E_F (3 states/eV atom) suggest ferromagnetic ordering on the surface, since a "Stoner" instability[13] can be easily

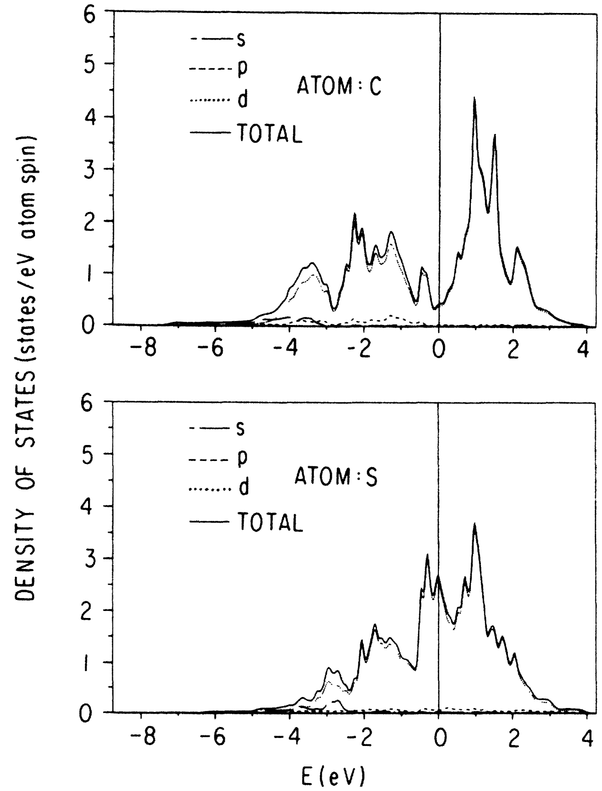

FIG. 3. Layer-projected and l-decomposed partial density of states in the units of states/eV atom in the paramagnetic state of a seven-layer Cr(001) film for the surface (S) and center (C) layer.

achieved even with an exchange integral assumed equal to the bulk value, 0.67 eV. [For[5] V(001), this sharp surface LDOS peak which is characteristic of the occurrence of surface magnetism in the 3*d* transition metals is located 0.3 eV above E_F. As a result, the paramagnetic state is more stable than the ferromagnetic state for V(001)]. As discussed earlier for[5] V(001), this high LDOS near E_F is dominated by prominent bands of surface states near the $\bar{\Gamma}$-$\bar{\Sigma}$-$\bar{M}$ symmetry line of the two-dimensional (2D) Brillouin zone. For paramagnetic Cr(001), these bands just cross E_F and a magnetic instability is induced for the surface atoms (Stoner theory). Consequently, large band splittings in the neighborhood of E_F as a result of ferromagnetic exchange interactions are expected for the ferromagnetic Cr(001) surface.

Figure 4 shows the calculated energy dispersion of the spin-up state (majority spin of surface atoms) [Fig. 4(a)], and spin-down state [Fig. 4(b)] of a seven-layer Cr(001) film along the high symmetry directions of the 2D Brillouin zone. The energy bands are sorted out for clarity into states with odd (upper panel) and even (lower panel) parities with respect to 2D rotational symmetry. States with even and odd parities with respect to *z* reflection are represented by dashed and dotted liens, respectively. Surface states, shown by solid curves, are defined as having their charge densities localized by more than 50% in the surface layer. Note that it is the occupied surface-state bands which have a predominantly majority-spin character. Normal-emission ARPES spectra at 300 K reported the existence of a prominent surface state with binding energy 0.65 eV (Ref. 26) and 0.75 eV (Ref. 12). As shown in Fig. 4(a), the result of our calculation also displays the same feature in the vicinity of the $\bar{\Gamma}$ symmetry point at an energy 1 eV below E_F. The increase of the calculated binding energy at 0 K compared with experiments at 300 K is consistent with the fact that the exchange splitting (and the binding energy of surface states for majority spin) increases with decreasing temperature. It is interesting to see the localization of surface states and band splitting along the symmetry line $\bar{\Gamma}$-$\bar{\Sigma}$-$\bar{M}$ (in particular, $\bar{\Sigma}_2$ symmetry). In W(001), a similar band splitting occurred as a result of a structural phase transition; in Cr(001) the band splitting is a consequence of a ferromagnetic phase transition on the surface.

In Fig. 5, the *l*-decomposed partial LDOS in the surface layer MT sphere, shown for the ferromagnetic state, reveals a large spin-density imbalance and gives rise to an enhancement of the local atomic moment to $2.49\mu_B$ per surface atom. In agreement with earlier studies,[12,13] our calculated ferromagnetic surface exchange splitting is found to be 1.8 eV. Normal-emission ARPES spectra at 300 K by Klebanoff *et al.*[12] display two surface-related features with binding energies of 0.16 eV (feature 1) and 0.75 eV (feature 2). They assign feature 2 to the surface resonance state of majority spin, and feature 1 is attributed to the manifestation of a rise in the minority surface DOS. He I photoemission studies by Zajac *et al.*[17] of Cr overlayers deposited on single-crystal Au(001) also display similar features: a broad peak with a binding energy of 1 eV and a shoulder near 0.1 eV; both of these features were identified as due to surface states. Indeed, in our calcula-

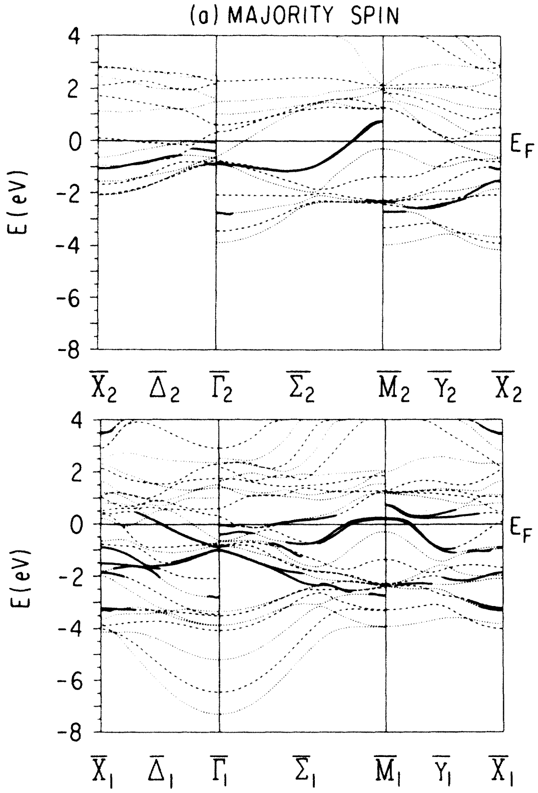

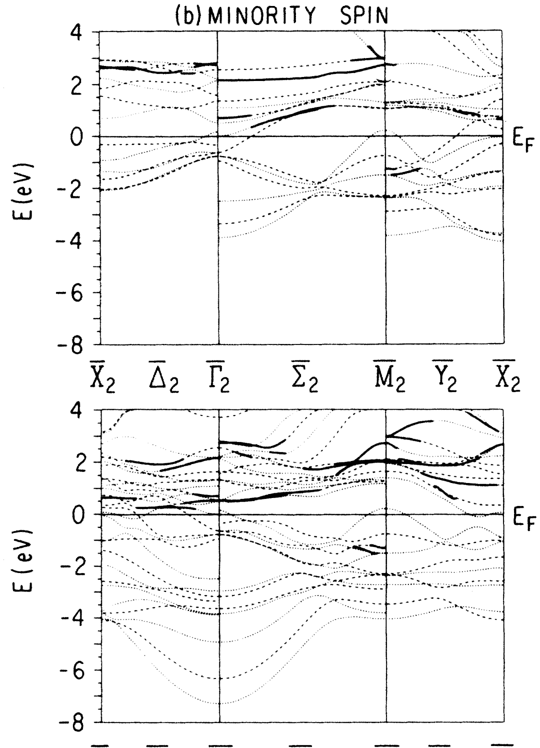

FIG. 4. Energy bands for a seven-layer Cr(001) film of majority spin, and minority spin along high symmetry directions in the 2D Brillouin zone. Top lower panels show odd and even symmetries, respectively, with respect to the 2D rotational symmetry, respectively. Dashed and dotted lines represent even and odd parities with respect to the *z* reflection. Solid lines indicate surface states whose wave functions have more than 50% weight within the surface layer.

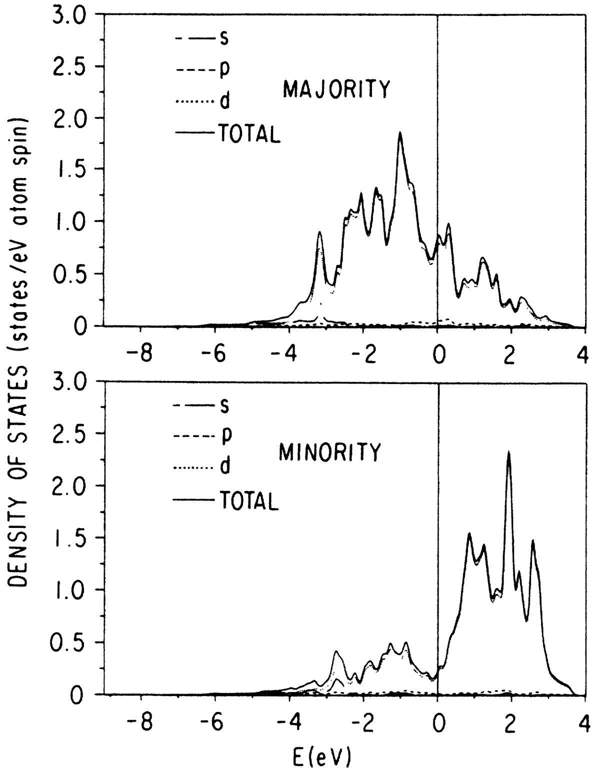

FIG. 5. Layer-projected and *l*-decomposed surface partial density of states in the units of states/eV spin atom for majority spin and minority spin of a seven-layer Cr(001) film.

tion a majority-spin LDOS peak with BE equal to 1 is clearly exhibited in Fig. 5(a), and is attributed to the surface state near $\bar{\Gamma}$ as discussed previously. In addition, a LDOS peak near (slightly above) E_F for majority spin is also seen in Fig. 5(a); the occupied portion of this feature may correspond to the shoulder (0.1 eV BE) in the photoemission spectra. This peak near E_F originates from the ferromagnetic exchange splitting of the paramagnetic surface state about 1 eV above E_F [cf. Fig. 3(b)]. In contrast, there is little evidence in our calculation that "feature 2" of Ref. 12 is of minority-spin character as suggested by Klebanoff *et al.* [cf. Fig. 5(b)].

IV. SUMMARY

We have presented the results of a self-consistent, all-electron local-spin-density-functional calculation on a seven-layer Cr(001) slab using the FLAPW method. The results show that whereas the charge density quickly approaches a bulklike environment only one layer below the vacuum-metal interface, the spin density has a larger screening length. The magnetic moments for the atoms in the surface layer and subsurface layer are enhanced to $2.49\mu_B$ and $-1.29\mu_B$, respectively; a bulklike antiferromagnetic coupling between $S-2$ and C layers is found. The contact hyperfine field for the surface atoms is also enhanced in magnitude with a predicted value of -73 kG. The theoretical work function, 4.05 eV, obtained for the first time for the Cr(001) surface, is smaller than in the paramagnetic phase and indicates the importance of magnetic ordering, which can be easily modified by surface impurities, on this electrostatic quantity.

In agreement with photoemission experiments, a prominent majority-spin surface state at $\bar{\Gamma}$ with a binding energy of 1 eV is found. In contrast, little evidence is seen in our calculation that the shoulder near 0.1-eV binding energy of photoemission spectra is of minority-spin character.

ACKNOWLEDGMENTS

This work was supported by the National Science Foundation (Grant No. DMR82-16543) and by a grant of computer time from its Office for Advanced Scientific Computing at the University of Minnesota Computing Center. We are grateful to S. D. Bader and G. Zajac for helpful discussions and to the University of Minnesota Computing Center for excellent service.

---

[1] E. Wimmer, H. Krakauer, M. Weinert, and A. J. Freeman, Phys. Rev. B **24**, 864 (1981).

[2] O. Jepsen, J. Madsen, and O. K. Andersen, Phys. Rev. B **26**, 2790 (1982); E. Wimmer, A. J. Freeman, and H. Krakauer, *ibid.* **20**, 3113 (1984).

[3] S. Ohnishi, A. J. Freeman, and M. Weinert, Phys. Rev. B **28**, 6741 (1983).

[4] L. N. Liebermann, D. R. Fredkin, and H. B. Shore, Phys. Rev. Lett. **22**, 639 (1969); L. N. Liebermann, J. Clinton, D. M. Edwards, and J. Mathon, *ibid.* **25**, 232 (1970).

[5] S. Ohnishi, C. L. Fu, and A. J. Freeman, J. Magn. Magn. Mater. **50**, 161 (1985).

[6] C. Rau and A. Schmalzbauer (unpublished).

[7] P. E. Ferguson, J. Appl. Phys. **49**, 2203 (1978).

[8] S. Matsuo and I. Nishida, J. Phys. Soc. Jpn. **49**, 1005 (1980).

[9] C. Rau and S. Eichner, Phys. Rev. Lett. **47**, 939 (1981).

[10] F. Meier, D. Pescia, and T. Schriber, Phys. Rev. Lett. **48**, 645 (1982).

[11] J. S. Foord, A. P. C. Reed, and R. M. Lambert, Surf. Sci. **129**, 79 (1983).

[12] L. E. Klebanoff, S. W. Robey, G. Liu, and D. A. Shirley, Phys. Rev. B **30**, 1048 (1984).

[13] G. Allan, Phys. Rev. B **19**, 4774 (1979).

[14] D. R. Grempel, Phys. Rev. B **24**, 3928 (1981).

[15] N. Hirashita, G. Yokoyama, T. Kambara, and K. I. Gondaira, J. Phy. F **11**, 2371 (1981).

[16] C. L. Fu, A. J. Freeman, E. Wimmer, and M. Weinert, Phys. Rev. Lett. **54**, 2261 (1985).

[17] G. Zajac, S. D. Bader, and R. J. Friddle (unpublished).

[18] U. von Barth and L. Hedin, J. Phys. C **5**, 1629 (1972).

[19] L. Hedin and B. I. Lundqvist, J. Phys. C **4**, 2064 (1971).

[20] D. D. Koelling and B. N. Harmon, J. Phys. C **10**, 3107 (1977).

[21] A. J. Freeman and R. E. Watson, in *Magnetism*, edited by G. T. Rado and H. Suhl (Academic, New York, 1965), Vol. IIA, p. 167.

[22] R. J. Wilson and A. J. Mills, Jr., Surf. Sci. **128**, 70 (1983).

[23] G. Shirane and W. J. Takei, J. Phys. Soc. Jpn. **17**, Suppl. BIII, 35 (1962).

[24] H. L. Skriver, J. Phys. F **11**, 97 (1981); T. Oguchi and A. J. Freeman (unpublished).

[25] J. Kubler, J. Magn. Magn. Mater. **20**, 277 (1980).

[26] G. Gewinner, J. C. Peruchetti, A. Jaegle, and R. Pinchaux, Phys. Rev. B **27**, 3358 (1983).